DESIGN AND FABRICATION OF AN INTEGRATED THREE-DIMENSIONAL TACTILE SENSOR FOR SPACE ROBOTIC APPLICATIONS

Tao Mei [1,2], Yu Ge [1], Yong Chen [1], Lin Ni [1], Wei-Hsin Liao [2], Yangsheng Xu [2] and Wen J. Li [2]

[1]*State Key Laboratories of Transducer Technology, Institute of Intelligent Machines, Chinese Academy of Sciences*
geyu@public.ustc.edu.cn

[2]*Department of Mechanical and Automation Engineering, The Chinese University of Hong Kong*
wen@mae.cuhk.edu.hk

ABSTRACT

An integrated three-dimensional tactile sensor with robust structure and soft contact surface suitable for space robotic applications was developed. The sensor has a maximum force range of 50N in the vertical direction and ±10N in the x-y horizontal directions. The sensitivity of the sensor cells in the vertical direction is 13mV/N and in the x and y horizontal directions are both 2.3mV/N. The tactile sensor includes 4x8 sensing cells each exhibiting an independent, linear response to the three components of forces. Post bulk-micromachining was performed on foundry fabricated CMOS chips to produce the sensor cells. With neural network training, the tactile sensor produced reliable 3-axes force measurements and repeatable response on tactile images. Design analysis, fabrication procedures, and experimental results are presented in this paper.

INTRODUCTION

Many tactile sensors have been developed to provide tactile sensing abilities for intelligent robots, tele-operational manipulators, and haptic interfaces [1,2]. These tactile sensors can detect normal forces applied on the tactile pixels for gripping force control and generate tactile images for gripping positioning and object recognition. However, besides acquiring tactile images and normal forces, knowledge of tangential forces is also critical for force control and slide-prevention during gripping to ensure mission success, and therefore, three-dimensional tactile sensors are needed.

Several three-dimensional tactile sensors have been developed using piezoresistive [3], capacitive [4], and optical [5] sensing elements. Some of these tactile sensors were fabricated by MEMS technology that integrated sensing elements and pre-processing circuits for compactness, but were too weak and fragile for most applications. For example, the force range of a capacitive tactile pixel is only 0.01N [4]. Other tactile sensors that were not produced by MEMS technology are typically bulky (for example, a CCD camera is needed in an optical tactile sensor [5]) or have limited spatial sensing resolution.

Non-robustness to the applied forces or bulkiness of size prevents these three-dimensional tactile sensors to become potentially useful in space robots. The reliability of space systems is a very important issue due to the high costs of space missions. Therefore, the robustness of tactile sensors must be improved to gain high component reliability. Furthermore, the costs of space missions are highly dependent on the payload weight (about US$260/g [6]), thus the tactile sensors must be compact or integrated to minimise the payload mass and match the size of compact space robots. Recent proposals for small/micro/nano satellites and micro rovers have raised the needs for space microrobots [7]. Although these microrobots truly require micron-scale sensors, millimeter-scale three-dimensional tactile sensors are urgently required by present space robotic systems.

We have developed a robust MEMS integrated three-dimensional tactile sensor with soft contact surface that can be potentially used for space robotic applications. The sensor uses an over-stop design to increase the range of applied force and has CMOS integrated piezoresistive sensing elements and pre-processing circuitry to reduce total sensor volume. The sensor is designed for a space robot test bed to provide multi-functional tactile sensing abilities. The basic sensor design and performance are given in the following sections.

STRUCTURAL DESIGN OF THE SENSOR

The integrated tactile sensor is constructed with five structural layers: rubber surface, force concentrating columns, sensing array, protection base, and circuit base as illustrated in Figure 1. A 2mm thick rubber surface is used for absorbing shock and protecting the inner devices. The rubber layer is glued on the top of the force concentrating columns by filling silicone rubber glue on the surfaces of the columns and the sensing array. The force concentrating columns are made by bulk silicon and positioned in the center of the tactile sensing cells. Since the columns are surrounded by silicone rubber, a soft silicone rubber layer is formed around the columns. This silicone rubber glue layer provides large glue surface for the rubber surface and prevents moving friction on the sensing array surface. Therefore, the sensor may achieve more robustness while

0-7803-5194-0/99/$10.00 ©1999 IEEE

concentrate most of the distributed tactile forces onto the center of the sensing cells in the tactile sensing array.

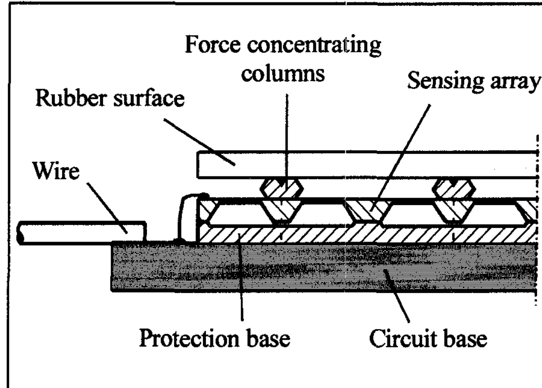

Figure 1. Illustration of the basic structures of the tactile sensor.

In the sensing array, there are 4×8 sensing cells that can detect three-dimensional forces. The sensing cell has an E-shape square membrane structure fabricated by silicon bulk micromachining. Strain induced by the applied forces on the membrane is sensed by three groups of integrated piezoresistors in the silicon membrane (Figure 2). The integrated sensing circuits used to detect F_x, F_y and F_z are shown in Figure 3. By strain and stress analysis of the E-shape membrane, suitable positions and shapes of the piezoresistors were determined to get optimal circuit outputs for F_x, F_y and F_z. When F_z is applied to the sensing cell, the stress and strain on the membrane where R_{x1}, R_{x2}, R_{y1}, and R_{y2} are located are theoretically equal, thus these piezoresistors have equal resistance change. Consequently, the outputs V_x and V_y of Circuit C_x and Circuit C_y have no response to F_z. However, under the load of F_z, R_{z1} and R_{z2} are under compressive stress while R_{z3} and R_{z4} are under tensile stress. Thus, R_{z1} and R_{z2} decrease while R_{z3} and R_{z4} increase under F_z, and the output V_z varies accordingly. When F_x is applied on the sensing cell, R_{x1} is compressed while R_{x2} is stretched, and the output V_x varies to respond to F_x. Also, R_{y1} and R_{y2} have the same resistance change in this case, so C_y has no response to F_x. The contributions from R_{z1} and R_{z2} are balanced in this case, since R_{z1} and R_{z2} are located on opposite but equal absolute value stress zones. For the same reason, the resistance change of R_{z3} and R_{z4} are balanced also. Therefore, V_z has no response to F_x. Similarly, when F_y is applied, V_y varies, but V_x and V_z have no response.

The protection base is a bulk-etched silicon substrate with predefined gaps to allow for the membrane deformation of the sensing cells, and is also designed to protect the membranes from excessive deformation. The maximum forces applied on the tactile sensor are 50N in Z direction and 10N in X and Y directions. These forces are distributed on all or some of the sensing cells.

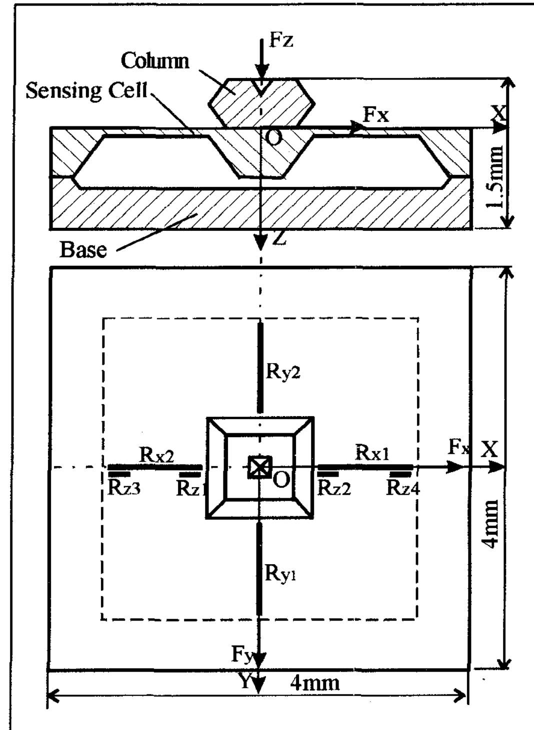

Figure 2. Locations of the piezoresistive elements of a three-dimensional force sensing cell.

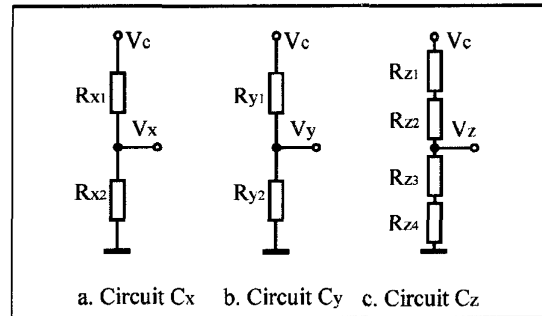

Figure 3. Force sensing circuits.

Theoretically, every sensing cell in the tactile sensor must be designed to have the same force range as the tactile sensor, since the total tactile force may be concentrated on a single sensing cell in the worst case. However, if the worst case scenario is taking into account, the sensitivity of sensing cell can not be maximised. A trade-off was made in designing the force range for the sensing cells. Usually, as observed from human behaviour, larger contact area is needed to apply large forces to get firm grip of an object. We

have assumed that robots can work in the same manner, i.e., if the force on a single cell exceeds the force range of that cell, the excess force is distributed to other cells on the tactile sensor. Therefore, we have designed the force range of the sensing cells to be 5N in Z direction and 1N in other directions. Since the stress and deformation under F_z are much bigger than F_x and F_y, the predefined gaps on the protection base can prevent over loading on the membranes.

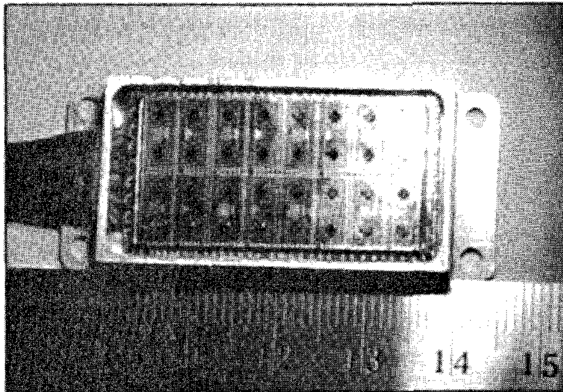

Figure 4. Photograph of the tactile sensor without the rubber surface.

Finally, the above four layers and the circuit base are assembled into a metal case to form a complete tactile sensor with $20\times50\times7mm^3$ total volume (Figure 4). The circuit base is made of a PCB circuit board for off-chip wiring. There are four holes on this metal case for attaching the tactile sensor to robot gripper surface by screws. The sensing area of the tactile sensor is $16\times32mm^2$ since each sensing cell is $4\times4mm^2$.

FABRICATION PROCEDURES

The tactile sensor was produced by four main processes: fabrication of small sensing cell array and the force overload-protection columns, micromachining of force concentrating column array, micromachining of protection base, and final assembling.

The fabrication of the small sensing cell array is the most important and difficult procedure since the array consists of integrated circuit and microstructures. If the total area of the sensing array is as large as $16\times32mm^2$, the yield rate for a single chip containing all 32 fully functional sensing cells will be relatively low after many complex processing steps. Smaller sensing chips with 2×2 cells in $8\times8mm^2$ area were fabricated, and the total tactile sensing array was composed by eight small chips. Every small chip has independent integrated circuit elements including piezoresistors, detection circuits, and analogue switches for data readout (Figure 5). Inter-chip and off-chip wire bonding contacts were patterned on every small chip, so any small chip could be placed in any position in the tactile sensing array.

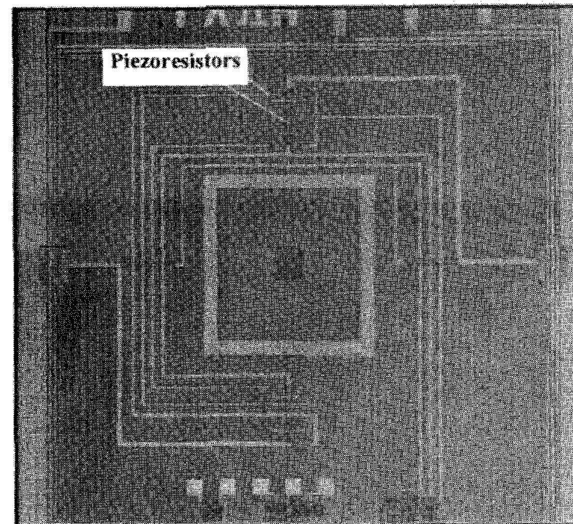

Figure 5. Micro-photograph of the piezoresistors and sensing circuits of a sensing cell.

The CMOS integrated sensor-circuit chips of the sensing array were fabricated at the East China Research Institute of Optical Electronics using double side polished 3-inch ⟨100⟩ silicon wafers. The doping concentration of the n-type silicon wafers is about $10^{15}/cm^3$. The piezoresistors were formed by injecting B^+ with $5.5\times10^{14}/cm^2$ dose, 100μA beam-current, 40keV for 35 seconds. The junction depths of the piezoresistors were diffused to about 1 μm by heating the wafers for 150 minutes under N_2 and 20 minutes under O_2 at 920°C. Standard CMOS processes were used to make the detection circuits and the analogue switches.

A backside photolithographic procedure was followed to open etching windows for the E-shape membranes. The CMOS circuits were protected and the chips were immersed in a 33% KOH solution at 76°C and time-etched to obtain 70μm thick membranes (Figure 6). Finally, the silicon chips were cut to $8\times8mm^2$ dice.

The force concentrating column array is initially composed of a frame with 4×8 columns connected by cantilevers. There are V-shape grooves at both ends of the cantilevers, so the cantilevers could be removed by applying a small force when the columns were glued to the center of the sensing cells. This way, the force concentrating columns could be easily handled, positioned and separated. The silicon column array was fabricated by the same bulk micromachining

process as the sensing cell array. The protection base was also made with silicon using the same technique.

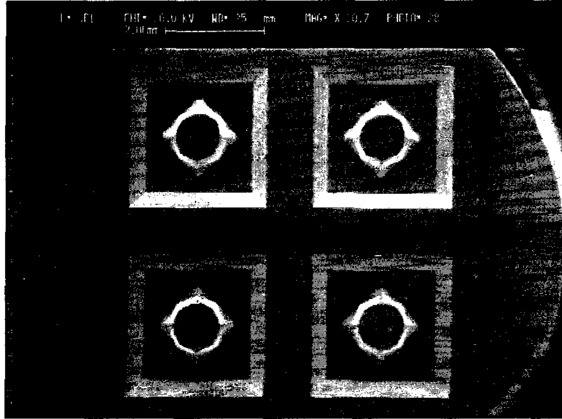

Figure 6. SEM picture of the E-shape membranes of four sensing cells.

The assembling process of the tactile sensor is described below. The procedure is illustrated in Figure 7.

a. Epoxy glue was coated on the protection base by thick film printing technique, and eight selected small sensing arrays were placed on the protection base. A 50g weight was applied on the top of the sensing array under 60°C for 4 hours to get firm connection.
b. Epoxy glue was printed on the center of the sensing array, and the force concentrating column array was aligned and pressed to the sensing array. Then, a 50g weight was applied on the top of the column array under 60°C for 4 hours to get firm connection.
c. Small forces were applied to break the cantilevers, then 32 columns separately stood on the center of the sensing cells after the cantilever frame is removed.
d. The assembly was aligned, pressed and glued to the circuit base by the same method as in steps *a* and *b*. Then, the inter-chip and off-chip wire bonding were performed.
e. Finally, the assembly was fixed in the metal case by epoxy glue, and the rubber layer was adhered to the top surface by silicone glue. After 24 hours of room temperature glue drying, the fabrication process is complete.

EXPERIMENT RESULTS

The sensing cells were calibrated to determine their sensitivity before silicone rubber was used to cover them. The test set-up is shown in Figure 8. A standard three-dimensional force sensor was used as the force reference, and was calibrated to 0.5% error by loading weights. The standard force sensor was fixed on a movable carriage in Z-direction and could be moved down to apply a Z-direction force to the cells. The tactile sensor was fixed on an X-Y table. The forces on X and Y directions could be applied by moving the tactile sensor in X and Y direction when the head of the standard force sensor was pressed on the surface. A small hole was fabricated on the center of the column surface to prevent sliding (see Figure 2). A set of sensitivity data for every cell in the array for the three force directions was obtained using this method. The sensitivity of the sensing cells were about 13mV/N in Z direction and about 2.3mV/N in X and Y directions.

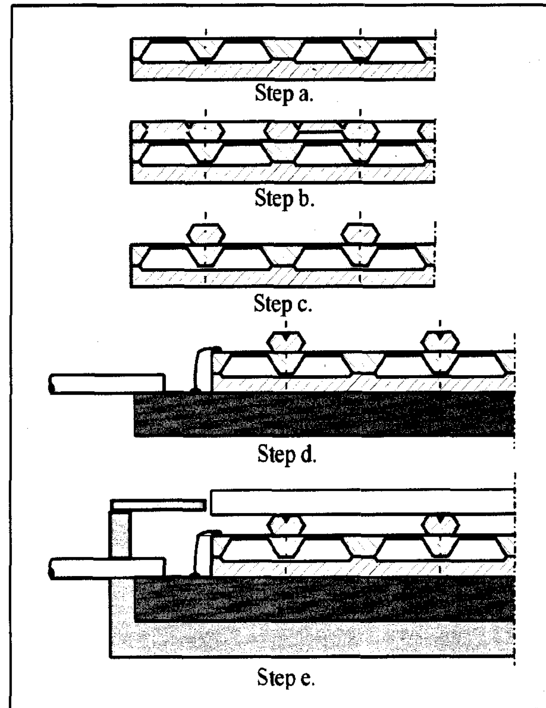

Figure 7. The tactile sensor assembling process.

The sensitivity of the individual sensing cells were affected by the silicone rubber layer covering the force concentrating columns. An artificial neural network was used to compensate the change, since theoretical analysis of the sensitivity change would be very complex. The neural network was a back-progression network with 97 input neurons, 32 hidden neurons and 3 output neurons. The 97 input neurons received the 32 three-dimensional forces and a temperature-sensing signal from the sensing array. A diode was integrated in the sensing circuit to detect the chip temperature for temperature compensation. The three output gave the total tactile forces in the three force directions. The mechanical analysis of the

multi-layer structure including the rubber layer, the E-shape membrane and silicon glue is an undergoing research issue. The tactile sensor was connected to the artificial neural network and trained by applying weights on the sensing surface directly. The tactile sensor achieved 2%FS accuracy for total tactile force measurements in the force range of 0 to 50 N for Fz and -10 to 10 N for Fx and Fy (Figure 9).

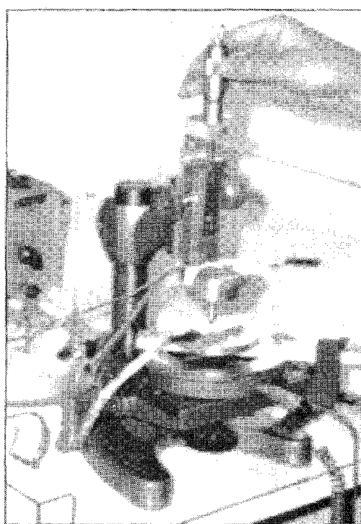

Figure 8. The experimental set-up for cell calibration

Some samples, such as keys, weights and screw nuts, were pressed to the tactile sensor to obtain tactile images. Good correspondence between the sample shapes and the force distribution were observed as shown in Figure 10.

CONCLUSION

An integrated three dimensional tactile sensor with novel force concentrating and overload-protection silicon columns was fabricated using MEMS and standard COMS technology. The sensor cells have integrated piezoresistors, detection circuits, and analogue switches for data readout. Reasonable detection accuracy of three force directions, tactile image correspondence, and the overall tactile sensor compactness and robustness were achieved. Integration of the tactile sensor is underway to a space test-bed robotic system.

ACKNOWLEDGEMENT

We would like to thank the Hong Kong UGC (Research Direct Grant #2050173) and High Technology Program of China for funding this research project.

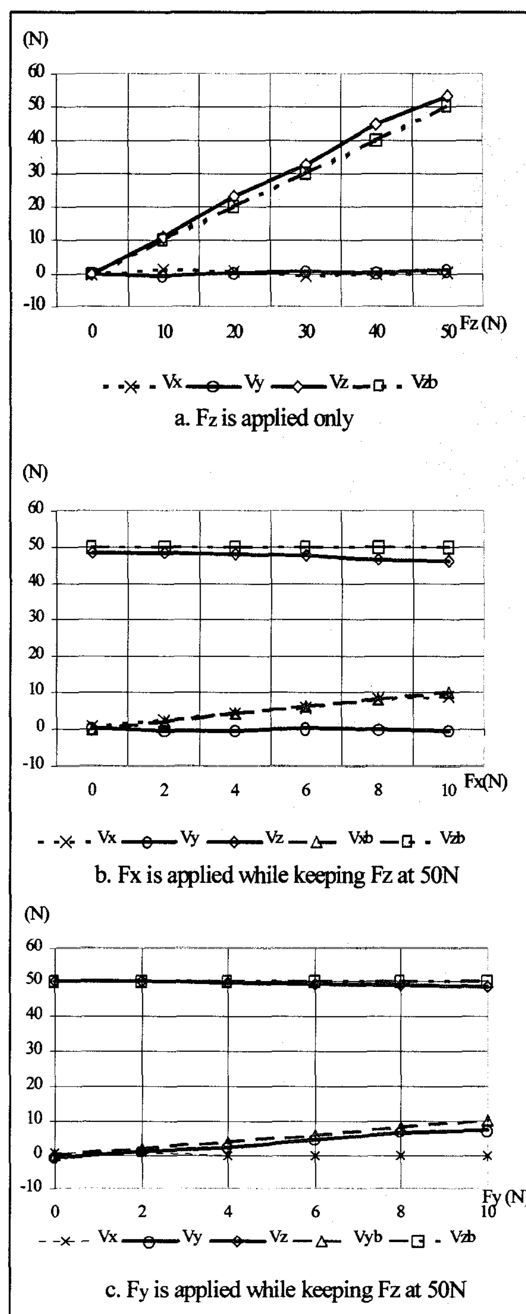

Figure 9. Input-output relationship of the three force components. (Note 1: Vxb, Vyb, Vzb are the ideal output curves. Note 2: Vxb, Vyb, and Vzb are the errors which are amplified by 10 times for clearness. Note 3: The output from the sensor have been mapped to forces by the neural net.)

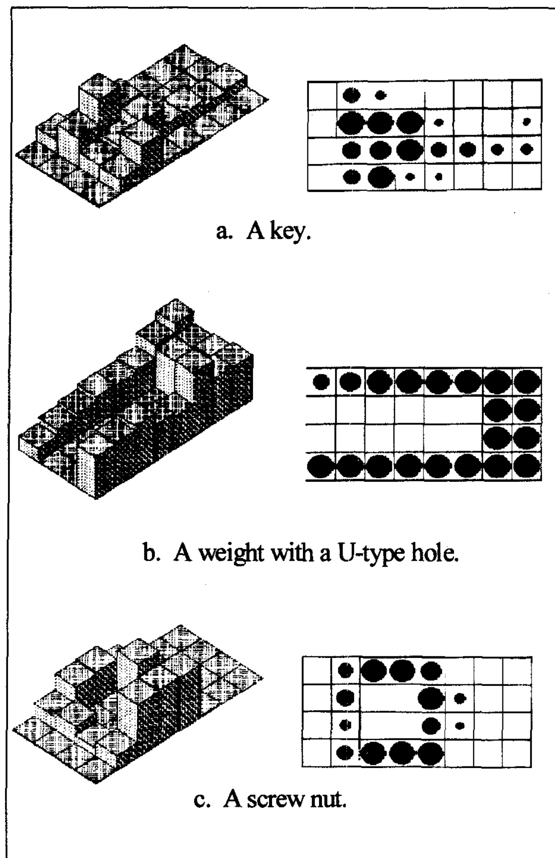

Figure 10. Tactile images with force and position distribution information.

REFERENCES

1. B. L. Gray and R. S. Fearing, *A surface micromachined microtactile sensor array,* Proceedings of IEEE International Conference on Robotics and Automation, ·Minneapolis, Minnesota, April 1996, pp. 1-6.
2. K. K. Choi, S. L. Jiang and Z. Li, *Multifingered robotic hands: contact experiments using tactile sensors,* Proceedings of the 1998 IEEE International Conference on Robotics and Automation, Leuven, Belgium, May 1998, pp. 2268-2273
3. B. J. Kane, M. R. Cutkosy and G. T. A. Kovacs, *CMOS-compatible traction stress sensor for use in high-resolution tactile imaging,* Sensors and Actuators, Vol. A54, 1996, pp. 511-516.
4. Z. Chu, P. M. Sarro and S. Middelhoek, *Silicon three-axial tactile sensor,* Sensors and Actuators, Vol. A54, 1996, pp. 505-510.
5. M. Ohka et al., *A three-axis optical tactile sensor (FEM contact analyses and sensing experiments using a large-sized tactile sensor),* Proceedings of IEEE International Conference on Robotics and Automation, Aichi, Japan, May 1995, pp. 817-824.
6. J. R. Wertz and W. J. Larson, *Reducing space mission cost,* Microcosm Press and Kluwer Academic Publishers, 1996
7. T. Mei, Y. S. Xu, W. H. Liao and W. J. Li, *Space microrobots: why, what, and how,* Second international Workshop on Micro Robotics and Systems, Beijing, China, October 1998, pp. 222-225.